Inorganic Chemistry

pubs.acs.org/IC Article

Amyloid β Perturbs Cu(II) Binding to the Prion Protein in a Site-Specific Manner: Insights into Its Potential Neurotoxic Mechanisms

Yanahi Posadas, Lili Parra-Ojeda, Claudia Perez-Cruz,* and Liliana Quintanar*

Cite This: https://doi.org/10.1021/acs.inorgchem.1c00846 Read Online

ACCESS | Metrics & More | Article Recommendations | Supporting Information

ABSTRACT: Amyloid β (Aβ) is a Cu-binding peptide that plays a key role in the pathology of Alzheimer's disease. A recent report demonstrated that Aβ disrupts the Cu-dependent interaction between cellular prion protein (PrP^C) and *N*-methyl-D-aspartate receptor (NMDAR), inducing overactivation of NMDAR and neurotoxicity. In this context, it has been proposed that Aβ competes for Cu with PrP^C; however, there is no spectroscopic evidence to support this hypothesis. Prion protein (PrP) can bind up to six Cu(II) ions: from one to four at the octarepeat (OR) region, producing low- and high-occupancy modes, and two at the His96 and His111 sites. Additionally, PrP^C is cleaved by α-secretases at Lys110/His111, yielding a new Cu(II)-binding site at the α-cleaved His111. In this study, the competition for Cu(II) between Aβ(1−16) and peptide models for each Cu-binding site of PrP was evaluated using circular dichroism and electron paramagnetic resonance. Our results show that the impact of Aβ(1−16) on Cu(II) coordination to PrP is highly site-specific: Aβ(1−16) cannot effectively compete with the low-occupancy mode at the OR region, whereas it partially removes the metal ion from the high-occupancy modes and forms a ternary OR-Cu(II)-Aβ(1−16) complex. In contrast, Aβ(1−16) removes all Cu(II) ions from the His96 and His111 sites without formation of ternary species. Finally, at the α-cleaved His111 site, Aβ(1−16) yields at least two different ternary complexes depending on the ratio of PrP/Cu(II)/Aβ. Altogether, our spectroscopic results indicate that only the low-occupancy mode at the OR region resists the effect of Aβ, while Cu(II) coordination to the high-occupancy modes and all other tested sites of PrP is perturbed, by either removal of the metal ion or formation of ternary complexes. These results provide important insights into the intricate effect of Aβ on Cu(II) binding to PrP and the potential neurotoxic mechanisms through which Aβ might affect Cu-dependent functions of PrP^C, such as NMDAR modulation.

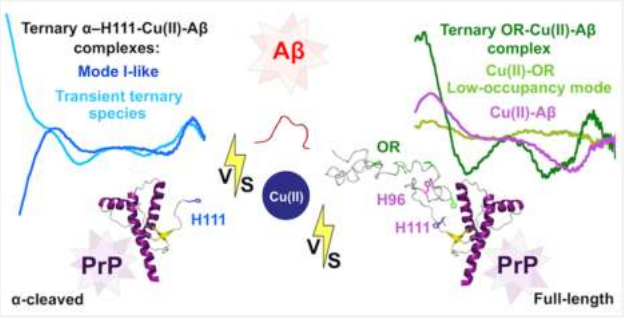

INTRODUCTION

Alzheimer's disease (AD) is a chronic neurodegenerative disorder that causes progressive cognitive decline.[1] The World Health Organization recognizes AD and other dementias as the seventh cause of death worldwide in 2019.[2] According to the World AD report 2015, there are 46.8 million people living with dementia, from which 60−70% of the cases correspond to AD.[3] Brain tissue from AD patients is characterized by extracellular accumulation of fibrillar amyloid β (Aβ) peptide, forming amyloid plaques.[1] Aβ is a Cu(II)-binding peptide produced by the sequential cleavage of the amyloid precursor protein (APP) by β- and γ-secretases.[4] Although Cu(II) coordination to Aβ is well-known, its physiological and pathological implications remain unclear.[4] AD patients and mice models show alterations in Cu homeostasis: this metal ion is accumulated in amyloid plaques,[5−8] decreased in degenerated brain regions,[9−11] and increased in serum.[12,13] Thus, it has been proposed that amyloid aggregates form a sink of Cu, contributing to the disruption of metal homeostasis and promoting oxidative stress.[14] Indeed, several in vitro studies show that the Cu(II)-Aβ complex produces reactive oxygen species, which might be involved in the oxidative damage observed in AD patients.[15] Hence, Cu removal from amyloid plaques has been proposed as a therapeutic approach to treat AD.[14] However, molecules that target metal ions have shown limited benefits for AD patients in clinical trials (phase II),[16,17] suggesting that the role of Cu(II)-Aβ interaction is beyond Cu accumulation in amyloid plaques and oxidative stress.[18]

Recently, another Cu-binding protein—the cellular prion protein (PrP^C)—was involved in a neurotoxic mechanism of Aβ that induces neuronal hyperexcitability.[19] PrP^C is a membrane-anchored protein, which is mainly expressed in the central nervous system (CNS), particularly in the pre- and postsynaptic compartments.[20,21] PrP^C has been associated with

Received: March 18, 2021

important cellular processes, such as memory and learning, neuritogenesis, neurogenesis, metal-ion homeostasis, and cell adhesion.[21] Although the mechanisms by which PrP^C is implicated in memory and learning are not well understood, it has been demonstrated that PrP^C modulates the *N*-methyl-D-aspartate receptor (NMDAR) in a Cu-dependent manner.[19,22] NMDAR is a ligand-gated calcium channel, the activation of which requires binding of Glu (the agonist) and Gly (the coagonist).[23] Ca entry through these receptors plays an important role in synaptic changes that occur during memory and learning acquisition;[24] however, NMDAR overactivation causes neurotoxicity,[25] and it has been associated with the neuronal hyperactivity observed in AD mice models and patients.[26,27] Indeed, memantine, an antagonist of NMDAR, is one of the four drugs currently approved to treat AD.[28] Two neuromodulation mechanisms of NMDAR activity that are Cu- and PrP^C-dependent have been proposed: reaction between nitric oxide (NO) and Cys residues at NMDAR and direct binding of PrP^C to NMDAR.[19,22] Both mechanisms induce a decrease in Ca currents through NMDAR and protect neurons from hyperexcitability.[19,22] Consistently, mice that are devoid of PrP^C or the Cu transporter ATP7A (copper-transporting P-type ATPase) show an increased susceptibility to neuronal damage by the overactivation of NMDAR.[29,30] Interestingly, Aβ and other Cu chelators promote cell death by disruption of the interaction PrP^C-NMDAR, suggesting that Aβ can compete for Cu with PrP^C.[19]

In the past decade, the coordination chemistry of Cu(II) binding to prion protein (PrP) and Aβ has been deeply characterized by several spectroscopic techniques.[31−34] At physiological pH, Aβ coordinates Cu(II) with high affinity (K_d ∼ 10 − 0.1 nM), displaying two coordination modes (Figure 1

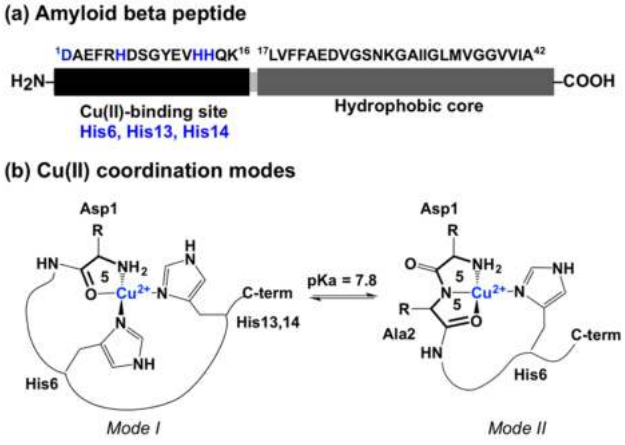

Figure 1. Cu(II) coordination to the Aβ peptide: (a) schematic representation of Aβ, showing the anchoring residues for Cu(II) at its N-terminal; (b) Cu(II) coordination modes proposed for modes I and II.[31]

b).[31,35] On the other hand, PrP can bind up to six Cu ions with different affinities (K_{ds} from 10 nM to 12 μM):[36,37] from one to four Cu(II) ions bind His residues at the region called octarepeat (OR),[37] which is constituted of an octapeptide (PHGGGWGQ) that is repeated four times, and two additional Cu(II) ions bind at His96 and His111 in the nonoctarepeat (non-OR) region (Figure 2a).[34,38]

Particularly, Cu(II) coordination at the OR region is highly dependent on the ratio of Cu(II)/PrP. When the concentration of Cu(II) is low (1:4 Cu/protein ratio), one Cu(II) is bound with high affinity (K_d ∼ 10 nM) using three or four His residues; this coordination mode is named component 3 or the low-occupancy mode (Figure 2b).[37,39] At a high concentration of Cu(II), each His residue can coordinate one Cu(II) ion with low affinity (K_d ∼ 7 to 12 μM), leading to coordination modes known as components 1 and 2 or high-occupancy modes (Figure 2c).[37,39]

At the non-OR region, Cu(II) is bound with a binding affinity (K_d ∼ 40−70 nM) that falls between of the low- and high-occupancy modes of the OR region.[40] The chemical environments around the Cu(II) ions bound at His96 and His111 are almost identical; in both cases, the Cu(II)-PrP complexes display two coordination modes: 3N1O and 4N modes (Figure 2d).[41,42] Interestingly, PrP^C is cleaved in the vicinity of the His111 site by ADAM8.[43−45] A high amount of α-cleaved PrP^C products have been detected in human brain, reaching up to 45% of the total PrP^C.[44] α-Cleavage of PrP^C occurs at Lys110/His111, yielding two fragments: N1 (Lys23−Lys110) that is released to the extracellular space and C1(His111−Ser230) that remains attached to the cellular membrane with a free NH_2 group at the N-terminal (Figure 3a).[46] N1 conserves intact the Cu(II)-binding sites at its OR region and His96, while C1 preserves His111 but lacks the residues that would provide the amide groups that participate in Cu(II) coordination to the full-length PrP.[47] Recently, the Cu(II) binding to a peptide that models the α-cleaved His111 site was studied by circular dichroism (CD), electron paramagnetic resonance (EPR), and NMR, revealing the formation of two different coordination modes that depend on the relative concentrations of Cu(II) and PrP.[47] Mode I is formed at low Cu(II) equiv (from 0.2 to 0.5), while mode II is observed from 0.6 to 1.0 equiv.[47] Interestingly, the formation of Cu(II)/peptide complexes in a ratio of 1:2 has been proposed for modes I and II (Figure 3b,c).[47] Unfortunately, there is no information about the Cu(II) binding affinity at the α-cleaved His111 site of PrP.

In order to dissect the effect of Aβ on the dynamic and complex Cu(II) coordination to PrP, we evaluated the competition for Cu(II) between Aβ(1−16) and peptide models for each metal-binding site at the OR and non-OR regions, as well as the α-cleaved His111 site, using EPR and CD.

RESULTS

Low-Occupancy, but Not the High-Occupancy, Mode at the OR Region Resists the Impact of Aβ(1−16). The low-occupancy mode or component 3 (Figure 2b) was prepared using a Cu(II)/PrP(60−91) ratio of 0.25:1.0 at pH 7.5, yielding a CD spectrum with no apparent signals (olive-green spectrum, Figure 4a), and an EPR spectrum with a set of signals with $g_{\|}$ = 2.260 and $A_{\|}$ = 190 × 10^{-4} cm^{-1} (olive-green spectrum, Figure 4b), consistent with previous reports.[37] Component 3 was titrated by Aβ(1−16) in order to evaluate the changes in Cu(II) coordination. Upon the addition of 2.0 equiv of Aβ(1−16), the EPR spectrum preserves the signals of component 3, including the characteristic N superhyperfine splitting at the perpendicular region (red spectrum, inset in Figure 4b). However, an EPR signal with $g_{\|}$ = 2.240 and $A_{\|}$ = 157 × 10^{-4} cm^{-1} is also present (red spectrum, Figure 4b and Table 1) and corresponds to a small amount of Cu(II) bound to Aβ(1−16). This is consistent with the presence of a weak-intensity CD signal at 31400 cm^{-1} (red spectrum, Figure 4a),

https://doi.org/10.1021/acs.inorgchem.1c00846
Inorg. Chem. XXXX, XXX, XXX−XXX

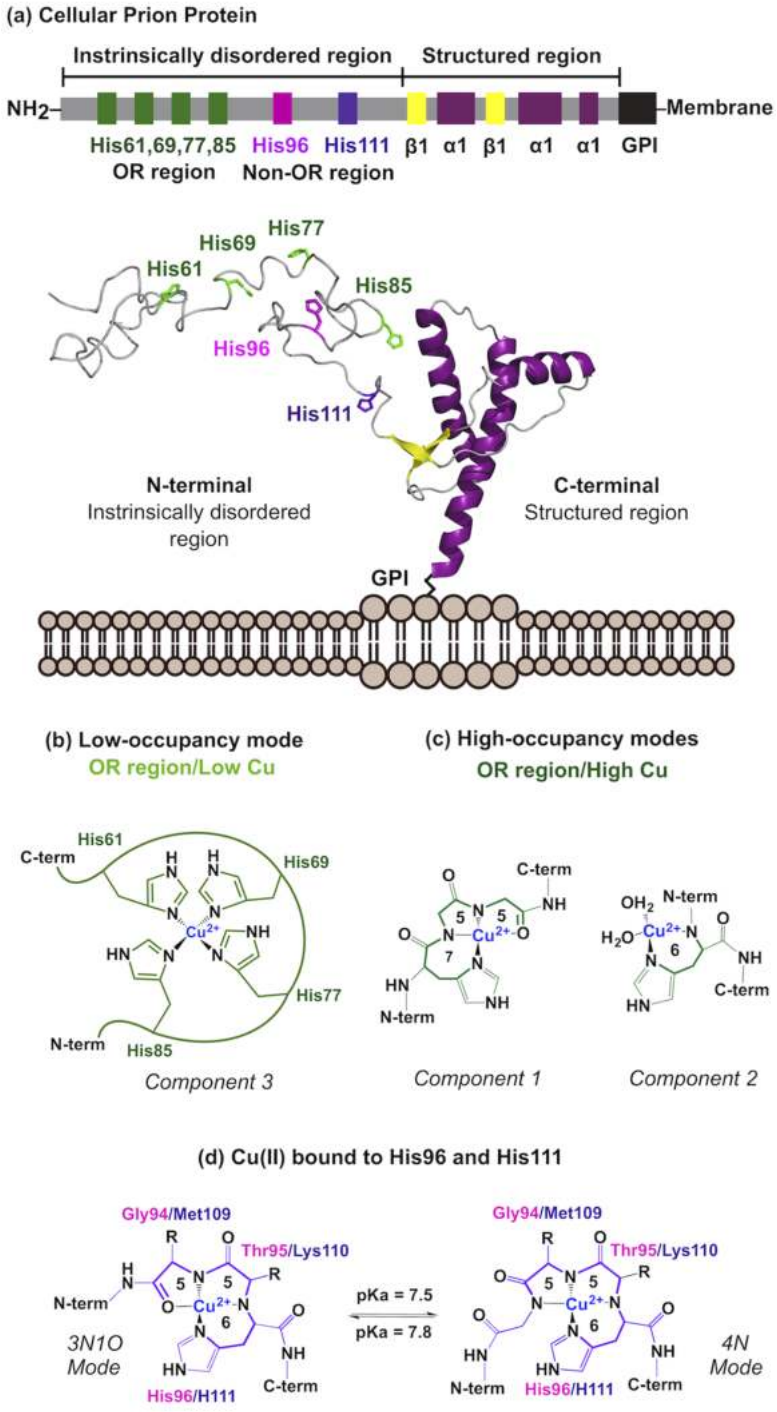

Figure 2. Cu(II) coordination to PrP: (a) schematic representation of PrP^C, showing the anchoring sites for Cu(II) at its N-terminal; (b–d) Cu(II)-coordination modes proposed for each metal-binding site at PrP.

associated with the deprotonated amide N^- to Cu(II) ligand-to-metal charge-transfer (LMCT) band observed in the Cu(II)-Aβ(1–16) complex.[48] To estimate the contribution of Cu(II)-Aβ(1–16) species, the spectra of component 3 and Cu(II)-Aβ(1–16) were added at different ratios, obtaining the best fit with 30% of Cu(II)-Aβ(1–16) and 70% of component 3 (dashed black lines, Figure 4). Thus, these results show that Aβ(1–16) cannot effectively take out Cu(II) from component 3, even when the concentration of Aβ(1–16) is 2-fold higher than that of PrP(60–91). Although the dissociation constants reported for Aβ(1–16) ($K_{dCuA\beta}$ ~ 10 – 0.1 nM)[35] and component 3 (K_{dCuC3} ~ 10 nM)[37] suggest that Aβ(1–16) has an equal or a higher affinity for Cu(II) than component 3, the formation constant of component 3 seems to be higher than that of the Cu-Aβ(1–16) complex; therefore, component 3 is the dominant species even at an excess of Aβ(1–16) under our experimental conditions.

https://doi.org/10.1021/acs.inorgchem.1c00846
Inorg. Chem. XXXX, XXX, XXX–XXX

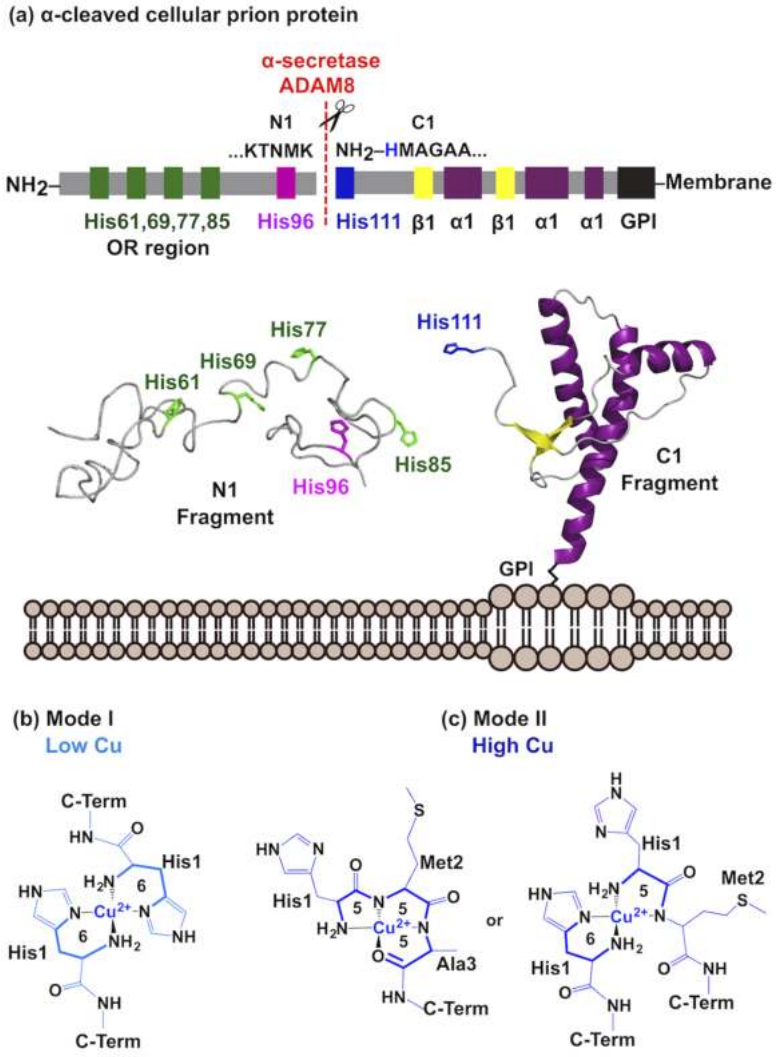

Figure 3. Cu(II) binding to the C1 fragment of the α-cleaved PrP: (a) schematic representation of PrP^C showing its α-cleavage site; (b and c) Cu(II)-coordination modes proposed for the α-cleaved His111 site of PrP.

The high-occupancy modes or components 1 and 2 (Figure 2c) were prepared using a Cu(II)/PrP(60−91) ratio of 2:1 at pH 7.5, displaying a CD spectrum with a high-intensity LMCT band at 29380 cm^{-1}, a positive d−d band at 17330 cm^{-1}, and a negative one at 14500 cm^{-1} (dark-green line, Figure 5a), which are characteristic signals of component 1.[49] Although component 2 is formed under these conditions, a previous report demonstrated that it is not CD-active.[37] The EPR spectrum shows two sets of signals: one with $g_{||}$ = 2.246 and $A_{||}$ = 169 × 10^{-4} cm^{-1} and another one with $g_{||}$ = 2.279 and $A_{||}$ = 170 × 10^{-4} cm^{-1} (dark-green spectrum, Figure 5b and Table 1), corresponding to components 1 and 2, respectively.[37] Also, the signals previously assigned to the Cu−Cu dipolar coupling between the component 1 centers are observed at $g_{||}$ = 2.18 and 1.94 (green asterisks, Figure 5b).[37] After the addition of 0.4 equiv of Aβ(1−16), the CD spectrum changes drastically (light-green line, Figure 5a) and the bands associated with component 1 decrease significantly, while two new signals become evident: a negative d−d band at 20270 cm^{-1} and a positive LMCT band at 31870 cm^{-1}. Consistently, in the parallel region of the EPR spectrum, the signals of component 1 decrease (light-green spectrum, Figure 5b); however, a set of signals with a $g_{||}$ value similar to that of component 3 appears (Figure S1b), and the N superhyperfine splitting becomes more evident (light-green line, inset in Figures 5b and S1b). It is important to note that the new CD signals are similar to those previously reported for a ternary OR_1-Cu(II)-Aβ(1−16) complex, where a single octapeptide (OR_1) that can only form component 1 yields stoichiometric formation of the ternary species.[50] Hence, a ternary OR_4-Cu(II)-Aβ(1−16) complex is formed under our conditions at the expense of component 1. However, in this study, the use of a peptide with four repeats of the octapeptide (OR_4) allows the formation of components 1−3, and thus only a small amount of the ternary OR_4-Cu(II)-Aβ(1−16) complex is formed at the expense of component 1, whereas the formation of component 3 is favored (light-green line, Figure S1b). Although this ternary complex is part of a mixture that includes components 1, 2 and 3, the latter two are not CD-active; thus, the CD spectrum of the ternary OR_4-Cu(II)-Aβ(1−16) species was obtained by the subtraction of reminiscent component 1 (Figure S2), yielding all of the characteristic signals of the previously reported OR_1-Cu(II)-Aβ complex: two d−d bands, a positive one at 15528 cm^{-1} and a negative one at 20149 cm^{-1}, as well as two LMCT bands at

https://doi.org/10.1021/acs.inorgchem.1c00846
Inorg. Chem. XXXX, XXX, XXX−XXX

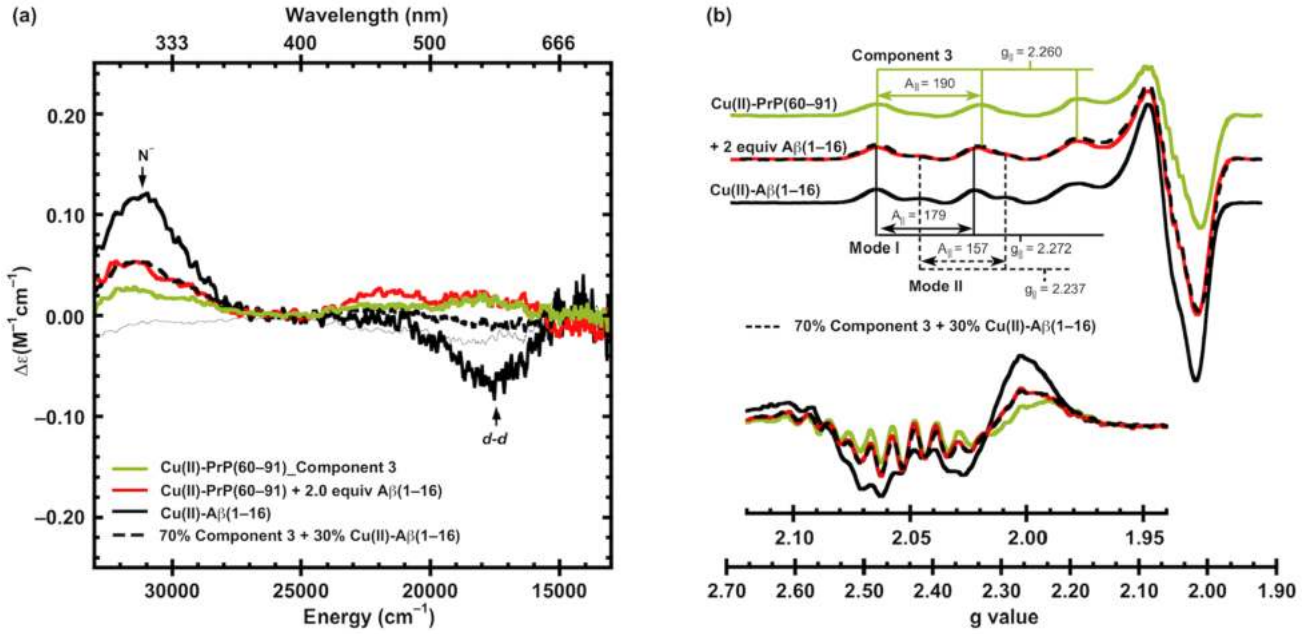

Figure 4. Titration of the low-occupancy mode of PrP or component 3 with Aβ(1−16), followed by CD (a) and EPR (b). Spectra of component 3 and Cu(II) bound to Aβ(1−16) are shown as olive-green and continuous black lines, respectively. The red spectra correspond to the titration of component 3 by 2.0 equiv of Aβ(1−16). Dashed black lines result from the addition of 30% of the Cu(II)-Aβ(1−16) spectra and 70% of the component 3 spectra. In the EPR spectra (b), the $A_{\parallel}$ values are given in 1×10^{-4} cm^{-1} and the inset shows the second derivative of the perpendicular region.

Table 1. EPR Parameters of Cu(II) Species Formed during Titrations of the Cu(II)-PrP Complexes by Aβ(1−16)[a]

sample	coordination mode	$g_{\parallel}$	$A_{\parallel}(1 \times 10^{-4}$ cm$^{-1})$	f factor (g_z/A_z)
Cu(II)-Aβ(1−16)	mode I	2.272	179	127
	mode II	2.237	157	142
Cu(II)-PrP(60−91)_low-occupancy mode	component 3	2.260	190	119
Cu(II)-PrP(60−91)_low-occupancy mode + 2.0 equiv of Aβ(1-16)	component 3	2.260	190	119
	Cu(II)-Aβ(1−16)_mode II	2.240	157	143
Cu(II)-PrP(60−91)_high-occupancy modes	component 2	2.279	170	134
	component 1	2.246	169	133
Cu(II)-PrP(60−91)_high-occupancy modes + 0.4 equiv of Aβ(1−16)	component 3	2.256	192	118
	component 1	2.236	167	134
Cu(II)-PrP(60−91)_high-occupancy modes + 1.0 equiv of Aβ(1−16)	mode I	2.265	183	124
	mode II	2.243	155	145
Cu(II)-PrP(60−91)_high-occupancy modes + 2.0 equiv of Aβ(1−16)	mode I	2.269	180	126
	mode II	2.238	156	143
Cu(II)-PrP(92−99)	3N1O/4N	2.228	184	121
Cu(II)-PrP(92−99) + 2.0 equiv of Aβ(1−16)	mode I	2.272	178	128
	mode II	2.243	157	143
Cu(II)-PrP(106−115)	3N1O/4N	2.226	178	125
Cu(II)-PrP(106−115)+ 2.0 equiv of Aβ(1−16)	mode I	2.274	173	131
	mode II	2.238	156	143
Cu(II)-PrP(111−116)	mode I	2.242	184	122
Cu(II)-PrP(111−116) + 2.0 equiv of Aβ(1−16)	ternary mode I-like complex	2.248	185	122
Cu(II)-PrP(111−116)	mode II	2.261	181	125
Cu(II)-PrP(111−116) + 2.0 equiv of Aβ(1−16)	ternary mode I-like complex	2.254	186	121
	Cu(II)-Aβ(1−16)			
	Cu(II)-PrP(111−115)_mode I			

[a]The parameters associated with mode I and a mode I-like complex were obtained from the EPR simulations shown in Figure S10.

27863 and 32303 cm^{-1}.[50] Moreover, the intensities of these CD signals are consistent with the formation of ∼0.4 equiv of the ternary complex (Figure S2). These spectroscopic data indicate that component 1 forms a ternary OR_4-Cu(II)-Aβ complex, and it might favor the population of component 3, even when the ratio of Cu(II)/OR is not significantly perturbed, suggesting that Aβ(1−16) has a significant impact on the equilibria between components 1−3.

https://doi.org/10.1021/acs.inorgchem.1c00846
Inorg. Chem. XXXX, XXX, XXX−XXX

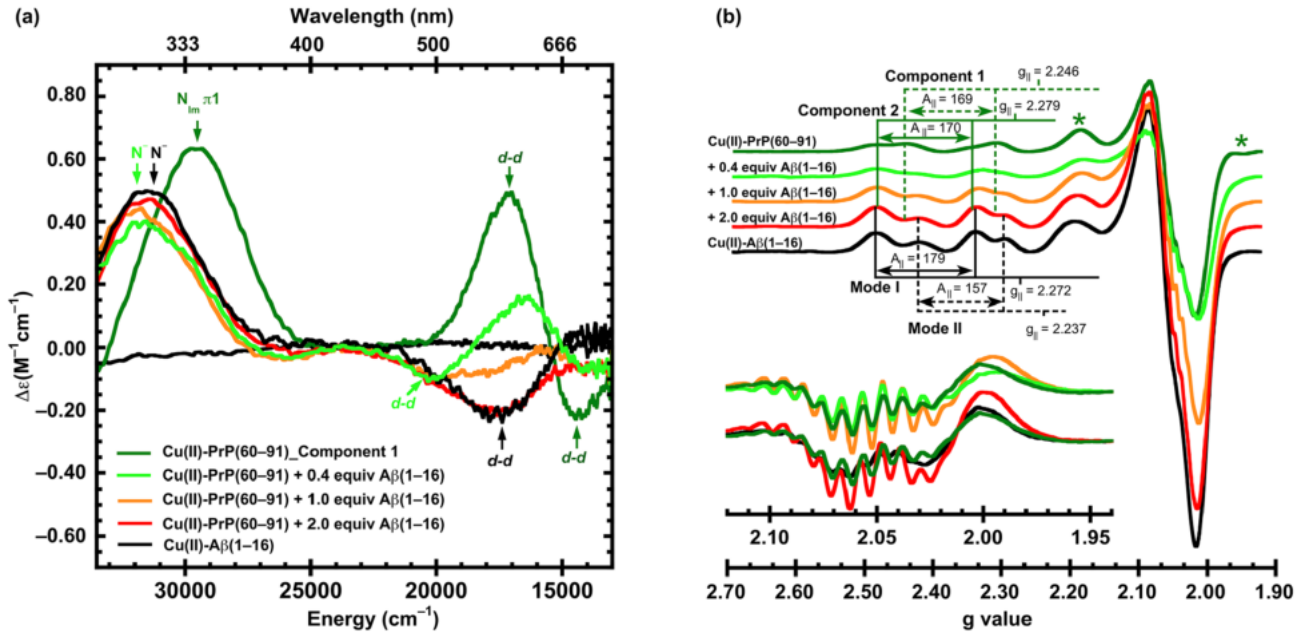

Figure 5. Titration of the high-occupancy modes Cu(II)-PrP(60−91) with Aβ(1−16) followed by CD (a) and EPR (b). The spectra of the high-occupancy modes and Cu(II) bound to Aβ(1−16) are shown as dark-green and continuous black lines, respectively. Light-green, orange, and red spectra correspond to titration of the high-occupancy modes by 0.4, 1.0, and 2.0 equiv of Aβ(1−16), respectively. In the EPR spectra (b), the $A_{\parallel}$ values are expressed in 1×10^{-4} cm^{-1} and inset shows the second derivative of the perpendicular region. Green asterisks point to the signals associated with the Cu−Cu dipolar coupling between the component 1 centers.

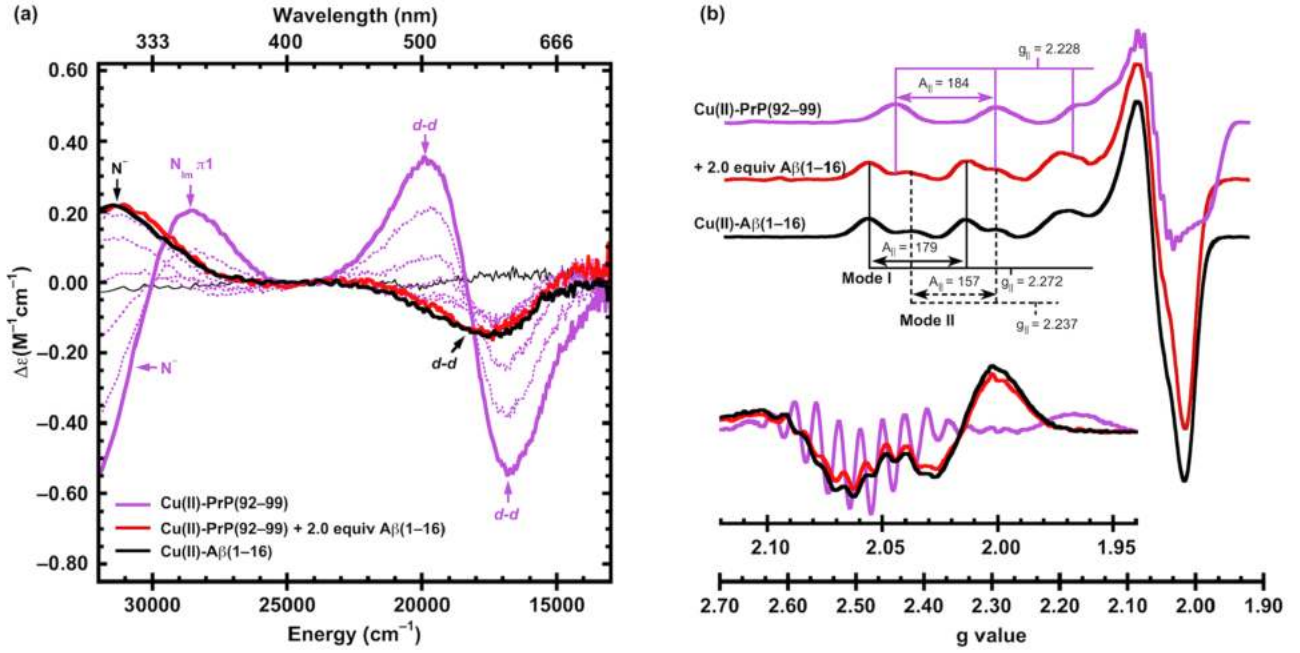

Figure 6. Titration of the Cu(II)-PrP(92−99) complex with Aβ(1−16) followed by CD (a) and EPR (b). The spectra of the Cu(II)-PrP(92−99) complex are shown as pink lines, dashed pink lines correspond to titration by Aβ(1−16) in aliquots of 0.2 equiv up to 1.0 equiv, and the red spectra result from the addition of 2.0 equiv of Aβ(1−16). The spectra of Cu(II) bound to Aβ(1−16) are included for comparison (continuous black lines). In the EPR spectra (b), the $A_{\parallel}$ values are expressed in 1×10^{-4} cm^{-1}, and the inset shows the second derivative of the perpendicular region.

Further additions of Aβ(1−16) to reach 1.0 equiv yield an EPR spectrum where modes I and II of the Cu(II)-Aβ(1−16) complex are clearly present (orange line, Figure 5b), while the intensity of the characteristic N superhyperfine splitting of component 3 increases (orange line, inset in Figure 5b). Interestingly, only small changes are observed in the CD spectrum in the ligand-field region, where the negative band associated with the ternary OR_4-Cu(II)-Aβ(1−16) species remains at 20149 cm^{-1} and the contribution of the negative d−d band of Cu(II)-Aβ(1−16) becomes evident (orange line,

https://doi.org/10.1021/acs.inorgchem.1c00846
Inorg. Chem. XXXX, XXX, XXX−XXX

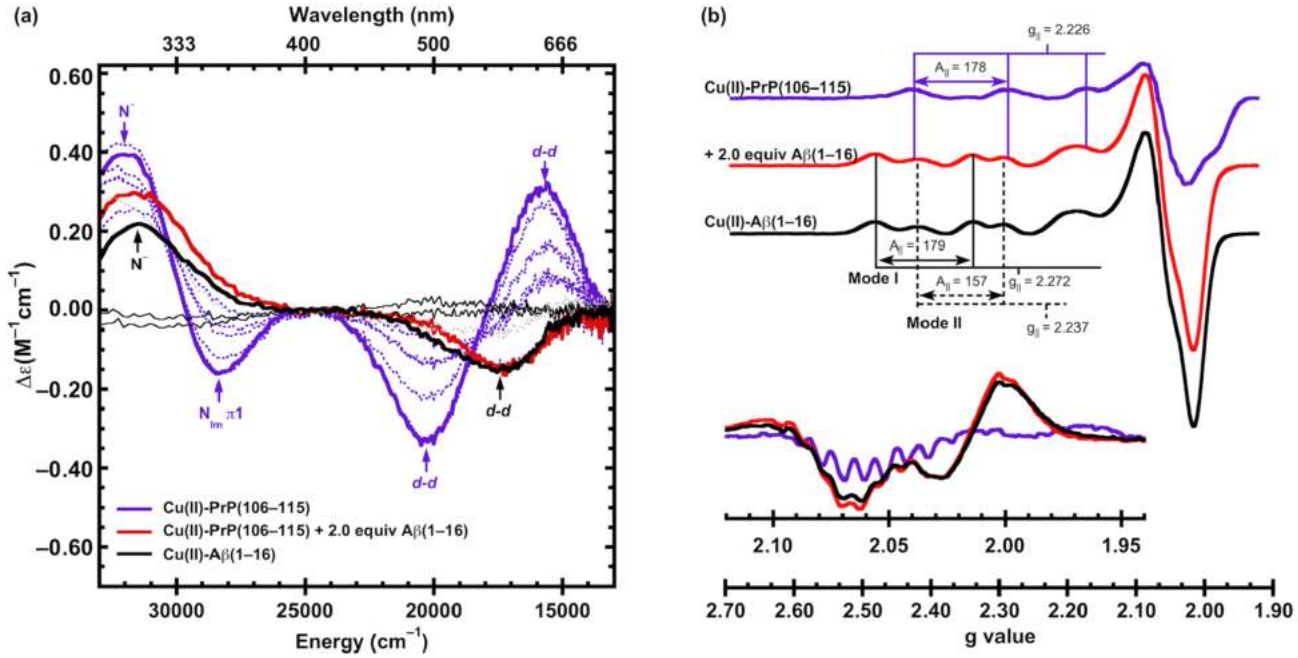

Figure 7. Titration of Cu(II)-PrP(106−115) complex with Aβ(1−16) followed by CD (a) and EPR (b). The spectra of Cu(II)-PrP(106−115) complex are showed in purple lines, dashed-purple lines corresponds to the addition of Aβ(1−16) in aliquots of 0.2 equiv up to 1.0 equiv, and the red spectrum results from the addition of 2.0 equiv of Aβ(1−16). The spectra of Cu(II)-Aβ(1−16) are included for comparison (continuous black line). In the EPR spectra (b), $A_{\parallel}$ values are expressed in 1×10^{-4} cm^{-1}, and inset shows the second derivative of the perpendicular region.

Figure 5a). After the addition of the second equiv of Aβ(1−16), the EPR and CD spectra are practically identical with those of the Cu(II)-Aβ(1−16) complex; however, the perpendicular region of the EPR spectrum still shows a N superhyperfine pattern reminiscent of component 3 (red spectra, inset in Figure 5b). To estimate the contribution of component 3 at the end point of the titration, the CD and EPR spectra of Cu(II)-Aβ(1−16) were added at different ratios, obtaining the best fit with 40% of component 3 and 60% of Cu(II)-Aβ(1−16), as shown in Figure S3.

Altogether, these results indicate that the effect of Aβ(1−16) on Cu(II) coordination at the OR region is highly pleomorphic: at a low Cu(II)/PrP ratio that favors component 3, Aβ(1−16) cannot effectively compete for Cu(II), while at a higher Cu(II)/PrP ratio, Aβ(1−16) partially competes for Cu(II) with the high-occupancy modes, forms a ternary complex at the expense of component 1, and perturbs the equilibria between the different Cu(II)-PrP species.

Aβ(1−16) Takes Cu(II) Away from the His96 and His111 Sites at the Non-OR Region. To study how Aβ(1−16) impacts Cu(II) coordination at the non-OR region, the His96 and His111 sites were modeled by the PrP(92−99) and PrP(106−115) fragments, respectively. The Cu(II)-PrP(92−99) complex at pH 7.5 displays a negative d−d band at 16718 cm^{-1} and a positive one at 19871 cm^{-1}, as well as a positive LMCT band at 28624 cm^{-1} and a negative one at 32388 cm^{-1} in the CD spectrum (pink spectrum, Figure 6a), while only a set of signals with $g_{\parallel}$ = 2.228 and $A_{\parallel}$ = 184 × 10^{-4} cm^{-1} was observed by EPR (pink lines, Figure 6b and Table 1). These signals correspond to a mixture of the 3N1O and 4N modes (Figure 2c), as previously reported.[41] Upon titration by Aβ(1−16), all CD signals associated with the Cu(II)-PrP(92−99) complex gradually decrease (dashed-pink lines, Figure 6a), whereas the CD signals of Cu(II) bound to Aβ(1−16) become evident with 1.0 and 2.0 equiv (red spectrum, Figure 6a). Consistently, the EPR spectrum of the end point of the titration is identical with that of the Cu(II)-Aβ(1−16) complex (red spectrum, Figure 6b). According to these results, Aβ(1−16) can effectively compete for Cu(II) with His96.

For the case of His111, Cu(II) bound to PrP(106−115) at pH 7.5 yields a CD spectrum with a positive d−d band at 15676 cm^{-1} and a negative one at 20277 cm^{-1}, as well as a negative LMCT band at 28305 cm^{-1} and a positive one at 32061 cm^{-1}, while a set of signals with $g_{\parallel}$ = 2.226 and $A_{\parallel}$ = 178 × 10^{-4} cm^{-1} is observed by EPR (pink lines, Figure 7 and Table 1). These signals are characteristic of a mixture of the 3N1O and 4N modes, as previously reported.[42] After the addition of increasing amounts of Aβ(1−16), all CD signals of the Cu(II)-PrP(106−115) complex decrease (dashed purple lines, Figure 7a), whereas a negative d−d band at 17320 cm^{-1} and a positive signal at 31450 cm^{-1} are clearly observed with 1.0 and 2.0 equiv (red spectrum, Figure 7a), both corresponding to the Cu(II)-Aβ(1−16) complex. Consistently, the EPR spectrum of the end point of the titration shows the characteristic signals of Cu(II) bound to Aβ(1−16) (red spectrum, Figure 7b), indicating that Aβ(1−16) can also take away Cu(II) from the His111 site.

Overall, these results show that the two non-OR binding sites lose Cu(II) in the presence of Aβ(1−16), which is consistent with the dissociation constants reported for His96 and His111 (K_d ∼ 40−70 nM)[40] and Aβ(1−16) (K_d ∼ 10 − 0.1 nM).[35]

Aβ(1−16) Forms Ternary Complexes at the α-Cleaved His111 Site. The peptide PrP(111−116) was used as a model of the α-cleaved His111 site. Mode I (Figure 3b) was prepared by adding 0.2 equiv of Cu(II) to PrP(111−116), displaying a CD spectrum with a negative LMCT band at 30606 cm^{-1} and a positive d−d transition at 14596 cm^{-1} (light-blue line, Figure

https://doi.org/10.1021/acs.inorgchem.1c00846
Inorg. Chem. XXXX, XXX, XXX−XXX

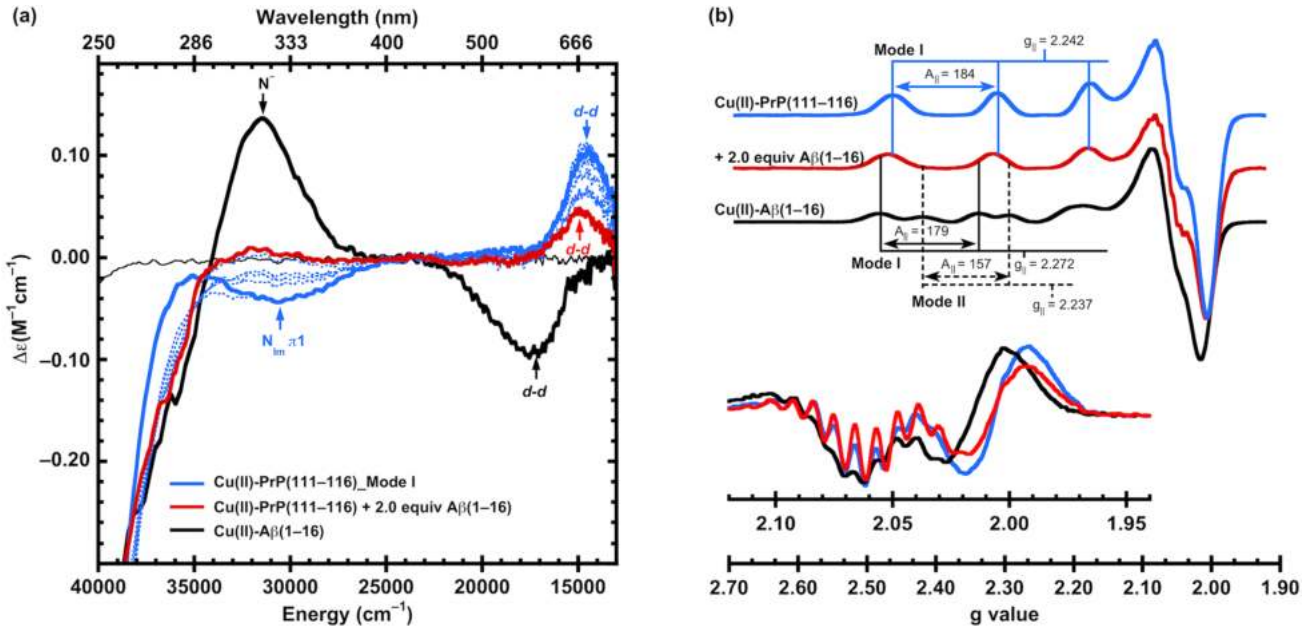

Figure 8. Titration of the complex Cu(II)-PrP(111−116) mode I with Aβ(1−16) followed by CD (a) and EPR (b). The spectra of mode I and Cu(II)-Aβ(1−16) are shown as continuous light-blue and black lines, respectively. Dashed light-blue spectra correspond to the addition of Aβ(1−16) in aliquots of 0.2 equiv up to 1.0 equiv, and the red spectra result by the addition of 2.0 equiv of Aβ(1−16). In the EPR spectra (b), the $A_{||}$ values are expressed in 1×10^{-4} cm^{-1}, and the inset shows the second derivative of the perpendicular region.

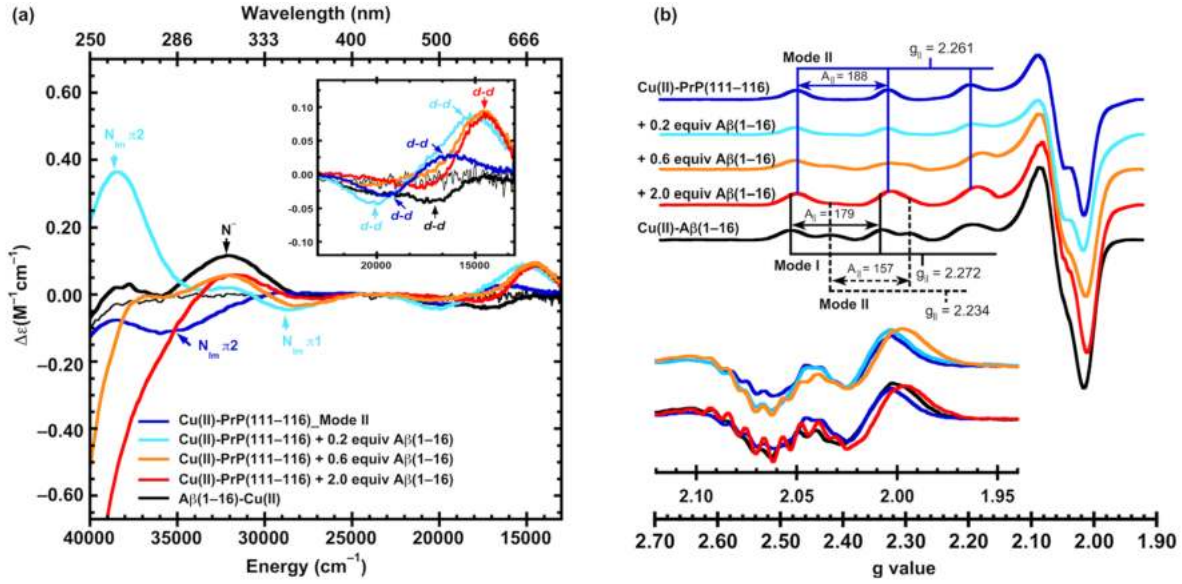

Figure 9. Titration of the complex Cu(II)-PrP(111−116) mode II with Aβ(1−16) followed by CD (a) and EPR (b). The spectra of the mode II and Cu(II)-Aβ(1−16) are shown as dark-blue and black lines. Light-blue, orange, and red spectra correspond to the titration of mode II by 0. 2, 1.0, and 2.0 equiv of Aβ(1−16), respectively. In the EPR spectra (b), the $A_{||}$ values are expressed in 1×10^{-4} cm^{-1}, and the inset shows the second derivative of the perpendicular region.

8a), as well as EPR signals with $g_{||}$ = 2.242 and $A_{||} = 184 \times 10^{-4}$ cm^{-1} (light-blue spectrum, Figure 8b and Table 1), consistent with the previous report.[46] Upon titration by Aβ(1−16), the signal associated with the LCMT imidazole π_1 to Cu(II) at 30606 cm^{-1} disappears, while the d−d band decreases in intensity and shifts to 14925 cm^{-1} (red line, Figure 8a). Consistently, at the end point of the titration, the $g_{||}$ value of the EPR signals shifts from 2.242 to 2.248 and the intensity of the N hyperfine splitting becomes more evident (red spectra, Figure 8b). No signals associated with the Cu(II)-Aβ(1−16) complex were detected. These results indicate that the chemical environment around Cu(II) changes upon the addition of Aβ(1−16), but it is different from the Cu(II)-Aβ(1−16) complex, suggesting the formation of a ternary α-His111-Cu(II)-Aβ species. Interestingly, this species shares some spectroscopic characteristics with mode I: a positive band around 14000−15000 cm^{-1} that indicates a low splitting of the d−d orbitals and an evident N superhyperfine pattern

https://doi.org/10.1021/acs.inorgchem.1c00846
Inorg. Chem. XXXX, XXX, XXX−XXX

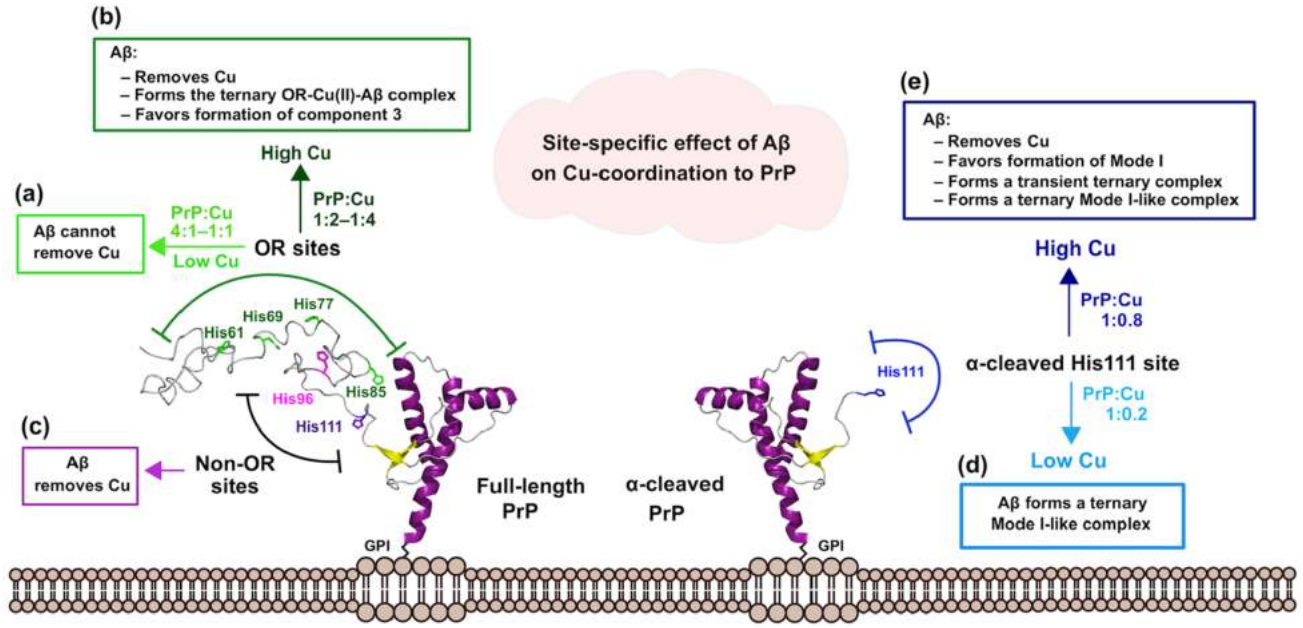

Figure 10. Effect of Aβ on Cu(II) coordination to metal-binding sites at full-length PrP (a–c) and α-cleaved PrP (d and e).

that suggests N-rich equatorial coordination. Hence, a new ternary mode I-like complex is formed.

Mode II (Figure 3c) was prepared using a Cu(II)/PrP(111–116) ratio of 0.8:1.0, yielding a CD spectrum with a negative LMCT band at 35061 cm^{-1}, a negative d–d transition at 19600 cm^{-1}, and a positive one at 16485 cm^{-1} (dark-blue line, Figure 9a), as well as a set of EPR signals with $g_{\parallel}$ = 2.261 and $A_{\parallel}$ = 181 × 10^{-4} cm^{-1} (dark-blue spectrum, Figure 9b and Table 1), consistent with the previous report.[46] Upon the addition of the first 0.2 equiv of Aβ(1–16), the CD spectrum changes drastically, the band at 35061 cm^{-1} disappears, and new signals are observed: a positive d–d band at 14555 cm^{-1} and a negative one at 20000 cm^{-1}, as well as three LMCT bands at 28277, 32072, and 38542 cm^{-1}, appear (light-blue line, Figure 9a). The resulting CD and EPR spectra do not seem to have a contribution from the Cu(II)-Aβ(1–16) complex. Although the EPR spectrum is dominated by mode II signals, small intensity changes are observed in the N superhyperfine region (light-blue line, inset in Figure 9b). These results indicate that a small amount of Aβ(1–16) significantly perturbs the nature of the Cu(II)-PrP(111–116) complex, possibly forming a ternary α-His111-Cu(II)-Aβ species, named the transient ternary complex. The CD spectrum of this ternary species was obtained by subtraction of reminiscent mode II from the light-blue spectrum (Figure S4).

Surprisingly, upon the addition of 0.6 equiv of Aβ(1–16), three of the signals associated with the transient ternary α-His111-Cu(II)-Aβ species almost disappear (the d–d band at 20000 cm^{-1} and the LMCT bands at 28277 and 38542 cm^{-1}, most notably that at 38542 cm^{-1}), while the d–d band at 14555 cm^{-1} remains present (orange spectrum, Figure 9a). Interestingly, the latter CD signal is reminiscent of the ternary mode I-like species described earlier. The EPR spectrum shows at least two sets of signals in the parallel region that are similar to mode II and the Cu(II)-Aβ(1–16) complex (orange spectrum, Figure 9b). This is consistent with the CD signal at 32072 cm^{-1} that corresponds to the Cu(II)-Aβ(1–16) complex (orange spectrum, Figure 9a); however, the CD and EPR spectra cannot be fitted by adding mode II and Cu(II)-Aβ(1–16) (Figure S5). At this point of the titration, there is a complex mixture that might include transient ternary α-His111-Cu(II)-Aβ species, ternary mode I-like species, mode I, and the Cu(II)-Aβ(1–16) complex (Figure S5).

Upon the addition of 2.0 equiv of Aβ(1–16), the characteristic CD signals of the transient ternary species disappear, while the signals associated with Cu(II) bound to Aβ(1–16) are clearly detected, and the positive d–d band at 14550 cm^{-1} that might correspond to mode I and the mode I-like complex is still observed (red spectrum, Figure 9a). Consistently, the EPR spectrum can be fitted as a mixture of Cu(II)-Aβ(1–16), mode I, and mode I-like species (Figure S6).

Overall, these results indicate that the effect of Aβ(1–16) on Cu(II) binding to the α-cleaved His111 site is highly dependent on the starting coordination mode: Aβ(1–16) addition to mode I quantitatively yields a ternary mode I-like species, which is also observed upon the titration of mode II by Aβ(1–16). However, in the latter, the formation of a transient ternary species is also observed. The formation of a ternary α-His111-Cu(II)-Aβ species suggests that Cu binding to the α-cleaved His111 site yields complexes that are more stable, compared to the uncleaved His111 site.

DISCUSSION

PrP^C is a Cu(II)-binding protein that is highly abundant in the CNS, particularly at the synaptic cleft,[20] where Cu is released in an activity-dependent manner[51] and reaches concentrations up to 100 mM.[52] Both PrP^C and Cu are involved in cellular processes that are key for the development and function of the CNS, such as modulation of Glu receptors,[19,22,53] neuritogenesis,[54] and memory and learning.[55–58] On the other hand, Aβ is a Cu(II)-binding peptide produced during normal neuronal activity,[59] which is found at low concentrations in the brains of cognitively normal individuals, but it is accumulated in AD.[60] The functional and pathological implications of the

https://doi.org/10.1021/acs.inorgchem.1c00846
Inorg. Chem. XXXX, XXX, XXX–XXX

Cu binding to PrP^C and Aβ remain unclear.[4,54] Previously, it was demonstrated that PrP^C modulates NMDAR in a Cu-dependent manner by direct binding to NMDAR, while Aβ and other Cu chelators disrupt this neuromodulator mechanism.[19] In the present study, the effect of Aβ(1−16) on Cu(II) coordination to the OR and non-OR sites was evaluated, as a first step to understanding how Aβ can impact the neuromodulation of NMDAR and other Cu-dependent roles of PrP^C.

Impact of Aβ on Cu-Binding Sites at the OR Region. The effect of Aβ(1−16) at the OR region depends on the relative concentrations of Cu(II) and PrP (Figure 10a,b). At low Cu(II) concentrations, Aβ(1−16) cannot remove more than 30% of Cu(II) from component 3, with this species being the only coordination mode that resists the effect of Aβ(1−16). Apparently, the multi-His macrochelate (component 3) is difficult to perturb, even when Aβ(1−16) provides good Cu(II)-anchoring sites (free NH_2 and His residues) that can yield to the formation of stable five-membered chelate rings (Figure 1b). Recently, it has been demonstrated that a coordination mode that is spectroscopically identical with component 3 is formed by three His residues from the OR region at the N-terminal and one His from the C-terminal in the full-length PrP.[61] This cis-interdomain interaction induced by Cu stabilizes a physiological conformation of PrP^C.[61] Our spectroscopic results suggest that Aβ would not disrupt the cis-interdomain contacts, leaving intact this physiologically protective interaction. However, it is important to note that the model used in this study does not include the C-terminal domain of PrP; thus, further spectroscopic and functional studies using the full-length PrP are required to evaluate the impact of Aβ on the cis-interdomain interaction.

At high Cu(II) concentrations, Aβ(1−16) has a pleomorphic impact on Cu(II) binding to PrP: it removes ∼60% of Cu(II) ions from the OR sites, forms a ternary OR_4-Cu(II)-Aβ(1−16) species with component 1, and induces the formation of component 3, even when this species is not favored by the Cu(II)/PrP ratio. These spectroscopic results suggest that Aβ can promote functions associated with low-occupancy modes at high Cu concentrations, while it could interfere with the functions associated with high-occupancy modes by removal of the metal ion and the formation of ternary species. Interestingly, the cellular localization of PrP^C is controlled by a mechanism that depends on Cu and OR sites.[62] PrP^C is found inside membrane microdomains, named lipid rafts, which have an important role in cellular signaling. The lateral movement of PrP^C out of lipid rafts is induced by a mechanism that requires high Cu concentrations and the OR region,[62] suggesting that the formation of high-occupancy modes (components 1 and 2) works as a switch that promotes dissociation of PrP^C from lipid rafts.[63] According to our spectroscopic results, Aβ(1−16) could prevent the movement of PrP^C out of lipid rafts by the removal of Cu from component 2 and the formation of ternary species with component 1. Moreover, dissociation of PrP^C from lipid rafts triggers PrP^C endocytosis,[62] which is necessary to activate important signaling pathways involved in learning and memory and neuritogenesis.[64,65] Thus, the impact of Aβ on the cellular localization of PrP^C could affect PrP^C endocytosis and its related functions.

Beyond the disruption of PrP^C functions associated with high-occupancy modes, the effect of Aβ on Cu(II) coordination to the OR region could have further impacts associated with the formation of ternary OR_4-Cu(II)-Aβ species. Therefore, understanding how Cu(II) induces the interaction between Aβ and PrP^C is crucial to dissecting the intricate relationship between these two Cu(II)-binding proteins. Further analysis of the spectroscopic features of the ternary OR_4-Cu(II)-Aβ(1−16) complex helps to identify the plausible ligands involved. The CD spectrum of this ternary species displays imidazole π_1 to Cu(II) and deprotonated amide to Cu(II) LMCT bands at 27863 and 32666 cm^{-1} (Figure 5a), revealing the presence of His residues and deprotonated amides in the coordination sphere. Moreover, the d−d transition at 20149 cm^{-1} suggests a large ligand-field splitting (Figure 5a), as expected when deprotonated amides are involved in Cu(II) coordination. Consistently, the d−d bands (20149 and 15528 cm^{-1}) with opposite signs resemble those observed in peptides that coordinate Cu(II) using His residues and deprotonated amides.[66,67] Interestingly, the CD spectrum of the ternary OR_4Cu(II)-Aβ(1−16) complex shares some characteristics with mode II of Cu(II) bound to Aβ(1−16), including the types of LMCT bands, energy, signs, and relative intensities of the two observed d−d transitions (Figure S7). In particular, the Cotton effect of the d−d bands has been empirically associated with a steric hindrance between the side chains of the residues that provide the deprotonated amides: bulky residues yield an intense negative d−d band at high energy and a positive one at low energy, as observed in the mode II of Cu(II) bound to Aβ(1−16), while Gly residues yield the inverse Cotton effect, as observed for component 1.[66] Thus, the similarity in the d−d bands of the ternary OR_4-Cu(II)-Aβ(1−16) complex and those of the Cu(II)-Aβ(1−16) complex suggests that the deprotonated amide is provided by Aβ(1−16), forming a stable five-membered chelate ring with the free NH_2, while PrP(60−91) could provide the His ligand. A proposal of the coordination mode of the ternary OR_4-Cu(II)-Aβ(1−16) complex is shown in Figure S8. Although further spectroscopic studies are required to identify unequivocally the ligands involved in this ternary species, this analysis provides important information to understand the kinds of interactions behind the formation of a ternary PrP-Cu(II)-Aβ complex. Even though PrP^C binds at least 45 different proteins,[68] the role of Cu in these interactions has barely been explored. According to our spectroscopic results, Aβ could interact with PrP^C in a Cu-dependent manner by the formation of a ternary PrP-Cu(II)-Aβ species at the OR region. Interestingly, the propensity of PrP^C to bind other molecules has been associated with its ability to activate signaling pathways.[68] Thus, functional studies are necessary to explore whether this ternary PrP-Cu(II)-Aβ species could have a role in signal transduction.

Impact of Aβ on the Cu Binding at the Non-OR Region. Aβ(1−16) completely removes Cu(II) ions from the His96 and His111 sites without the formation of ternary species (Figure 10c). In contrast to component 1 at the OR region, the anchoring His residue at the non-OR sites is followed by at least one bulky side chain, which possibly prevents the formation of ternary species by steric hindrance. Hence, Aβ can only affect PrP^C functions that require Cu(II) bound to the His96 and His111 sites by removal of the metal ion but not by the formation of ternary species. Interestingly, Aβ disturbs the Cu-dependent interaction of PrP^C with NMDAR in a manner identical with that of Cu chelating agents, and this effect is reversible,[19] suggesting that Aβ alters the PrP^C−NMDAR binding by removal of the metal ion.

https://doi.org/10.1021/acs.inorgchem.1c00846
Inorg. Chem. XXXX, XXX, XXX−XXX

According to our spectroscopic results, the His96 and His111 sites are the only sites that can lose Cu(II) to Aβ without the formation of ternary species, pointing to the non-OR sites as the plausible metal-binding region involved in the interaction between PrP^C and NMDAR. This is consistent with the metal-binding affinity of the His96 and His111 sites ($K_d \sim 40-70$ nM)[40] and the Cu concentrations (100 nM) used in the study that characterized the PrP^C-NMDAR interaction.[19] Therefore, Aβ accumulation can contribute to the aberrant activation of NMDAR by the removal of Cu(II) from the non-OR sites and disruption of the PrP^C–NMDAR binding. Interestingly, Aβ oligomers (Aβo) bind this same region of PrP^C, forming a protein complex that includes another Glu receptor (mGluR5, metabotropic glutamate receptor 5) that triggers the Fyn signaling pathway.[69] Aβ can also impact the other neuromodulator mechanism of NMDAR that depends on Cu and PrP^C, and it involves S-nitrosylation of Cys residues at the receptor.[22] However, the redox activity of Cu-PrP complexes is highly dependent on the coordination mode.[70] Thus, further spectroscopic and reactivity studies are necessary to identify the Cu-binding site(s) of PrP that can activate NO for S-nitrosylation of NMDAR and may be impacted by Aβ.

Overall, it is important to note that complex cellular processes, such as neuritogenesis and memory and learning, might involve more than one Cu- and PrP-dependent mechanism that could be affected by Aβ through removal of the metal ion and/or the formation of ternary species. However, with Aβ being another Cu-binding peptide evolutionary conserved and necessary for normal neuronal activity,[59] its plausible role as a modulator of mechanisms that depend on Cu and PrP^C cannot be ruled out.

Aβ Forms Ternary Complexes at the α-Cleaved PrP His111 Site. Beyond the dynamic Cu(II) coordination to PrP^C at the OR and non-OR regions that display several coordination modes with different metal-binding affinities, Cu(II) coordination to PrP^C can also be modulated by proteolytic processing.[47] PrP^C undergoes proteolytic cleavage by α-secretases at Lys110/His111, yielding a new Cu(II)-binding site at the C1 fragment that remains attached to the cellular membrane (Figure 3a).[47] Here, the effect of Aβ(1−16) on Cu(II) coordination to the α-cleaved His111 site was evaluated as a first step to understanding how Aβ can impact cellular functions that depend on Cu binding to the C1 fragment.

Similar to the OR region, the effect of Aβ(1−16) on the α-cleaved His111 site depends on the relative concentration of Cu(II) and PrP (Figure 10d,e). At low Cu concentrations that favor mode I, the addition of Aβ(1−16) yields a ternary α-His111-Cu(II)-Aβ(1−16) complex, termed the mode I-like complex. This species shares some spectroscopic features with mode I, suggesting that it binds Cu(II) using a ligand set with similar chemical nature. Mode I has been proposed as a complex formed by two molecules of PrP(111−115) per Cu(II) ion, involving two histidine residues and two NH_2 groups (Figure 3b), that resemble a histamine-like coordination mode. Like mode I, the CD spectrum of a ternary mode I-like complex displays an intense negative LMCT band around 40000 cm^{-1}, indicative of NH_2 group coordination (Figure 8a). Both PrP(111−116) and Aβ(1−16) could provide the NH_2 groups. The negative CD signal associated with LMCT from imidazole π_1 to Cu(II) in mode I is not present in the ternary mode I-like species (Figure 8a); however, the d−d bands of these complexes suggest a similar ligand-field splitting. The absence of imidazole π_1-to-Cu(II) LMCT in the ternary mode I-like complex could be due to the participation of His residues from Aβ(1−16) and PrP(111−116), yielding CD signals with opposite Cotton effects, as occurs in the individual Cu(II)-Aβ(1−16) and PrP(111−116) complexes. A proposal of the coordination mode of the ternary mode I-like complex is shown in Figure S9. Consistently, EPR simulations reveal rhombic environments for both mode I and ternary mode I-like species (Figure S10), which is in agreement with a coordination mode that involves two trans NH_2 groups and two trans His residues (Figure S9). The rhombicity of the Cu site arises from having an approximate D_{2h} symmetry that allows for d_{z^2} mixing into the $d_{x^2-y^2}$ ground state; from the g_x and g_y values for mode I and the ternary mode I-like complex, ≈2% of d_{z^2} mixing can be estimated, with minimal tetrahedral distortion according to the f factor (Table 1).[71] In both cases, a superhyperfine pattern is evident in the second derivative of the EPR spectrum that can be simulated by considering the coupling of four N nuclei (Figure S10 and Table S4). However, EPR simulations reveal that the slight differences in the N superhyperfine patterns of the two complexes are due to having different N superhyperfine coupling values: while mode I can be simulated with two sets of two magnetically equivalent N atoms with $^{N}A_{iso}$ = 45 and 28 MHz, the ternary mode I-like species requires different couplings for each N (Table S4). The two N atoms with higher coupling values can be assigned to two His ligands, having $^{N}A_{iso}$ values in the 40−43 MHz range, while the other two N-based ligands correspond to two NH_2 terminal groups, with $^{N}A_{iso}$ values ranging between the 34 and 37 MHz range (Table S4), consistent with the previously reported values.[72] The less symmetric N coupling interactions observed in the ternary mode I-like complex reflect that these ligands are provided by two different peptides. Taken together, these results support the notion of a ternary α-His111-Cu(II)-Aβ(1−16) species with a histamine-like coordination, where a His residue and a free NH_2 are provided by Aβ(1−16) and a second set is provided by PrP(111−116). Aβ(1−16) may stabilize this ternary species by the negative charge from Asp-1 or by the plausible participation of Asp-1 as an axial ligand (Figure S9). Hence, Aβ can disrupt cellular processes that require Cu-induced interaction between two C1 fragments by formation of the ternary mode I-like species. Moreover, the Cu(II)-induced binding of Aβ with the membrane-bound C1 fragment could activate a signaling pathway, as was observed with the binding of Aβ oligomers to full-length PrP^C.[69] Even though there are no identified functions that depend on mode I formation, it could be involved in cell adhesion and cell signaling.[46,73−75] PrP^C homophilic interactions are involved in cell adhesion between neurons at the synapse[73] and between endothelial cells at the blood−brain barrier,[74] while dimerization of C1 fragments at the same cellular membrane could activate a signaling pathway, as observed with other membrane proteins.[76]

At high Cu concentrations that favor mode II, the addition of 0.2 equiv of Aβ(1−16) yields a ternary species, named the transient ternary α-His111-Cu(II)-Aβ(1−16) complex. Interestingly, this species displays a CD spectrum similar to those observed in the ternary OR_4-Cu(II)-Aβ(1−16) complex, suggesting a similar Cu(II) coordination (Figure S11) that involves deprotonated amides, His residues, and free NH_2 groups. Both PrP(111−116) or Aβ(1−16) could provide deprotonated amides and free NH_2 groups to the coordination sphere of the transient ternary α-His111-Cu(II)-Aβ(1−16)

https://doi.org/10.1021/acs.inorgchem.1c00846
Inorg. Chem. XXXX, XXX, XXX−XXX

complex, yielding the proposed Cu(II) coordination mode shown in Figure S12. It is important to note that the transient α-His111-Cu(II)-Aβ(1−16) ternary complex is most abundant at 0.2 equiv of Aβ(1−16). At higher Aβ concentrations, ∼40% of Cu(II) is bound to Aβ(1−16), favoring mode I and thus formation of the ternary mode I-like complex. Hence, formation of the transient ternary α-His111-Cu(II)-Aβ(1−16) complex is favored under conditions with low amounts of Aβ, and it could perturb functions that depend on mode II.

The propensity of the α-cleaved His111 site to form ternary species is not observed in the His111 site of full-length PrP, suggesting that the presence of a free NH_2 group and a His residue in the first position provides a less sterically hindered environment that favors the formation of ternary species with Aβ. Moreover, the orientations of the NH_2 group and His residues (trans NH_2 and trans His) reduce the steric hindrance, which may be caused by the bulky side chains at the N-terminal of Aβ(1−16). These particular Cu(II)-binding properties of the α-cleaved His111 site could promote the formation of ternary species with other proteins or peptides with a free NH_2 group and good anchoring residues at the N-terminal, as demonstrated here for the case of Aβ. The Cu(II)-coordination properties of α-cleaved PrP^C open a myriad of potential roles of Cu in cell signaling and cell adhesion that could be perturbed by Aβ.

CONCLUDING REMARKS

Overall, our spectroscopic study demonstrates that the effect of Aβ on Cu(II) coordination to PrP is site-specific. At the OR region, the low-occupancy mode resists the effect of Aβ, indicating that any functional mechanism associated with this coordination mode would be resistant to Aβ. In contrast, the effect of Aβ on the high-occupancy modes is pleomorphic: It partially removes the metal ion, forms ternary OR_4-Cu(II)-Aβ species, and perturbs the equilibria between components 1−3. Thus, Aβ could alter cellular mechanisms that depend on components 1 and 2, such as the dissociation of PrP^C from lipid rafts and its functional implications. Moreover, the Cu-induced interaction between PrP and Aβ by the formation of ternary OR_4-Cu(II)-Aβ species could activate a signaling pathway, as observed with the binding of Aβ oligomers to full-length PrP^C.[69] On the other hand, Aβ completely removes Cu(II) from His96 and His111 without the formation of ternary species, pointing to the non-OR sites as the plausible metal-binding region involved in the Cu-dependent binding of PrP^C to NMDAR.

For the α-cleaved His111 site, our spectroscopic results show that it has a particular propensity to form ternary α-His111-Cu(II)-Aβ complexes that are not observed at the noncleaved protein. Formation of these ternary species with the membrane-attached C1 fragment of PrP^C could disrupt its potential role in cell adhesion or modulate signaling pathways, such as mitogen-activated protein kinase signaling.[75] Moreover, the spectroscopic features of ternary α-His111-Cu(II)-Aβ complexes suggest that the α-cleaved His111 site could form ternary species with other proteins that provide a free NH_2 group and good anchoring residues at the N-terminal. These results provide valuable insights into the identification of new molecules that could activate Cu-dependent signaling pathways through the α-cleaved PrP^C.

The multiple functional roles of Cu(II) coordination to PrP^C indicate that disruption of Aβ homeostasis can trigger several neurotoxic mechanisms associated with perturbed Cu(II)-PrP^C interactions. However, the coexistence of Aβ and PrP^C at the synaptic clefts under physiological conditions and the evolutionary selection of these two Cu(II)-binding proteins point to the role of Aβ in the modulation of PrP^C functions. Here, we have provided new insights into the complexity of the bioinorganic chemistry of Cu involved in AD, which is important not only to understanding the pathological role of Aβ but also to the redesign of therapeutical strategies that target metal ions to combat AD. Moreover, the differential effect of Aβ revealed in this study can be useful to distinguish the functional role of each Cu-coordination mode of PrP^C in cellular models.

ASSOCIATED CONTENT

Supporting Information

The Supporting Information is available free of charge at https://pubs.acs.org/doi/10.1021/acs.inorgchem.1c00846.

Materials and methods, peptides synthesized (Table S1), purification programs (high-performance liquid chromatography, HPLC) (Table S2), programs for purity testing (HPLC) (Table S3), titration of the high-occupancy modes by 0.4 equiv of Aβ(1−16) favoring the formation of component 3 (Figure S1), titration of the high-occupancy modes by 0.4 equiv of Aβ(1−16) forming a ternary OR_4-Cu(II)-Aβ(1−16) species that is similar to the previously reported octapeptide-Cu(II)-Aβ(1−16) complex (Figure S2), addition of 2.0 equiv of Aβ(1−16) to the high-occupancy modes (components 1 and 2) yielding a mixture of component 3 and Cu(II) bound to Aβ(1−16) (Figure S3), titration of the PrP(111−116)-Cu(II) mode II by 0.2 equiv of Aβ(1−16), forming a transient ternary α-His111-Cu(II)-Aβ(1−16) complex (Figure S4), titration of the Cu(II)-PrP(111−116) mode II by 0.6 equiv of Aβ(1−16), forming a complex mixture of Cu complexes (Figure S5), titration of the complex Cu(II)-PrP(111−116) mode II with 2.0 equiv of Aβ(1−16), yielding a mixture of mode I, mode I-like complex, and Cu(II)-Aβ(1−16) (Figure S6), comparison between mode II of Cu(II) bound to Aβ(1−16) and the ternary OR_4-Cu(II)-Aβ(1−16) complex (Figure S7), Cu(II)-coordination mode proposed for the ternary OR_4-Cu(II)-Aβ(1−16) complex (Figure S8), Cu(II)-coordination mode proposed for the ternary mode I-like complex (Figure S9), simulations of the EPR spectra of mode I (a) and the ternary mode I-like complex (b) (Figure S10), parameters used to simulate the EPR spectra of mode I and the ternary mode I-like complex (Table S4), titration of the Cu(II)-PrP(111−116) mode II by 0.2 equiv of Aβ(1−16), forming a transient ternary complex with spectroscopic features similar to those of the ternary OR_4-Cu(II)-Aβ(1−16) complex (Figure S11), and Cu(II)-coordination modes proposed for the transient ternary α-His111-Cu(II)-Aβ(1−16) species (Figure S12) (PDF)

AUTHOR INFORMATION

Corresponding Authors

Claudia Perez-Cruz − *Department of Pharmacology, Center for Research and Advanced Studies (Cinvestav), 07360 Mexico City, Mexico;* orcid.org/0000-0002-5983-307X; Email: cperezc@cinvestav.mx

https://doi.org/10.1021/acs.inorgchem.1c00846
Inorg. Chem. XXXX, XXX, XXX−XXX

Liliana Quintanar − *Department of Chemistry, Center for Research and Advanced Studies (Cinvestav), 07360 Mexico City, Mexico;* orcid.org/0000-0003-3090-7175; Email: lilianaq@cinvestav.mx

Authors

Yanahi Posadas − *Department of Chemistry and Department of Pharmacology, Center for Research and Advanced Studies (Cinvestav), 07360 Mexico City, Mexico;* orcid.org/0000-0003-2480-4233

Lili Parra-Ojeda − *Department of Chemistry, Center for Research and Advanced Studies (Cinvestav), 07360 Mexico City, Mexico*

Complete contact information is available at: https://pubs.acs.org/10.1021/acs.inorgchem.1c00846

Funding

This research was supported by SEP-Cinvestav funds from the Ministry of Education and by the National Council for Science and Technology in Mexico (CONACYT) through Grant 221134, a undergraduated fellowship to Lili Parra-Ojeda (24473), and a graduate fellowship to Yanahi Posadas (308512).

Notes

The authors declare no competing financial interest.

■ ACKNOWLEDGMENTS

The authors are grateful to Atenea Villegas Vargas and Gabina Dionisio Cadena for their invaluable technical assistance in peptide synthesis and Geiser Cuellar for acquisition of the mass spectra to characterize the peptide fragments used in this study. The authors are also grateful to Prof. Paolo Carloni (INM-9, Forschungszentrum Jülich) for providing molecular-simulation-derived structures of the N-terminal of PrP used for schematic representations of PrP^{C}.

■ REFERENCES

(1) DeTure, M. A.; Dickson, D. W. The neuropathological diagnosis of Alzheimer's disease. *Mol. Neurodegener.* **2019**, *14* (1), 32.

(2) Organization, W. H. Causes of Death, https://www.who.int/news-room/fact-sheets/detail/the-top-10-causes-of-death, 2019.

(3) Prince, M. W. A.; Guerchet, M.; Ali, G. C.; Wu, Y.-T.; Prina, M. *World Alzheimer Report 2015. The Global Impact of Dementia. An analysis of prevalence, incidence, costs and trends*; Alzheimer's Disease International: London, 2015.

(4) Kepp, K. P. Alzheimer's disease: How metal ions define β-amyloid function. *Coord. Chem. Rev.* **2017**, *351*, 127−159.

(5) Lovell, M. A.; Robertson, J. D.; Teesdale, W. J.; Campbell, J. L.; Markesbery, W. R. Copper, iron and zinc in Alzheimer's disease senile plaques. *J. Neurol. Sci.* **1998**, *158* (1), 47−52.

(6) Wang, H.; Wang, M.; Wang, B.; Li, M.; Chen, H.; Yu, X.; Yang, K.; Chai, Z.; Zhao, Y.; Feng, W. Immunogold labeling and X-ray fluorescence microscopy reveal enrichment ratios of Cu and Zn, metabolism of APP and amyloid-beta plaque formation in a mouse model of Alzheimer's disease. *Metallomics* **2012**, *4* (10), 1113−8.

(7) Miller, L. M.; Wang, Q.; Telivala, T. P.; Smith, R. J.; Lanzirotti, A.; Miklossy, J. Synchrotron-based infrared and X-ray imaging shows focalized accumulation of Cu and Zn co-localized with beta-amyloid deposits in Alzheimer's disease. *J. Struct. Biol.* **2006**, *155* (1), 30−7.

(8) James, S. A.; Churches, Q. I.; de Jonge, M. D.; Birchall, I. E.; Streltsov, V.; McColl, G.; Adlard, P. A.; Hare, D. J. Iron, Copper, and Zinc Concentration in Abeta Plaques in the APP/PS1Mouse Model of Alzheimer's Disease Correlates with Metal Levels in the Surrounding Neuropil. *ACS Chem. Neurosci.* **2017**, *8* (3), 629−637.

(9) Deibel, M. A.; Ehmann, W. D.; Markesbery, W. R. Copper, iron, and zinc imbalances in severely degenerated brain regions in Alzheimer's disease: possible relation to oxidative stress. *J. Neurol. Sci.* **1996**, *143* (1−2), 137−42.

(10) Magaki, S.; Raghavan, R.; Mueller, C.; Oberg, K. C.; Vinters, H. V.; Kirsch, W. M. Iron, copper, and iron regulatory protein 2 in Alzheimer's disease and related dementias. *Neurosci. Lett.* **2007**, *418* (1), 72−6.

(11) Xu, J.; Church, S. J.; Patassini, S.; Begley, P.; Waldvogel, H. J.; Curtis, M. A.; Faull, R. L. M.; Unwin, R. D.; Cooper, G. J. S. Evidence for widespread, severe brain copper deficiency in Alzheimer's dementia. *Metallomics* **2017**, *9* (8), 1106−1119.

(12) Bucossi, S.; Ventriglia, M.; Panetta, V.; Salustri, C.; Pasqualetti, P.; Mariani, S.; Siotto, M.; Rossini, P. M.; Squitti, R. Copper in Alzheimer's disease: a meta-analysis of serum, plasma, and cerebrospinal fluid studies. *J. Alzheimer's Dis.* **2011**, *24* (1), 175−85.

(13) Li, D. D.; Zhang, W.; Wang, Z. Y.; Zhao, P. Serum Copper, Zinc, and Iron Levels in Patients with Alzheimer's Disease: A Meta-Analysis of Case-Control Studies. *Front. Aging Neurosci.* **2017**, *9*, 300.

(14) Lei, P.; Ayton, S.; Bush, A. I. The Essential Elements of Alzheimer's Disease. *J. Biol. Chem.* **2021**, *296*, 100105.

(15) Cheignon, C.; Tomas, M.; Bonnefont-Rousselot, D.; Faller, P.; Hureau, C.; Collin, F. Oxidative stress and the amyloid beta peptide in Alzheimer's disease. *Redox Biol.* **2018**, *14*, 450−464.

(16) Ritchie, C. W.; Bush, A. I.; Mackinnon, A.; Macfarlane, S.; Mastwyk, M.; MacGregor, L.; Kiers, L.; Cherny, R.; Li, Q. X.; Tammer, A.; Carrington, D.; Mavros, C.; Volitakis, I.; Xilinas, M.; Ames, D.; Davis, S.; Beyreuther, K.; Tanzi, R. E.; Masters, C. L. Metal-protein attenuation with iodochlorhydroxyquin (clioquinol) targeting Abeta amyloid deposition and toxicity in Alzheimer disease: a pilot phase 2 clinical trial. *Arch. Neurol.* **2003**, *60* (12), 1685−91.

(17) Lannfelt, L.; Blennow, K.; Zetterberg, H.; Batsman, S.; Ames, D.; Harrison, J.; Masters, C. L.; Targum, S.; Bush, A. I.; Murdoch, R.; Wilson, J.; Ritchie, C. W. Safety, efficacy, and biomarker findings of PBT2 in targeting Abeta as a modifying therapy for Alzheimer's disease: a phase IIa, double-blind, randomised, placebo-controlled trial. *Lancet Neurol.* **2008**, *7* (9), 779−86.

(18) Drew, S. C. The Case for Abandoning Therapeutic Chelation of Copper Ions in Alzheimer's Disease. *Front. Neurosci.* **2017**, *11*, 317.

(19) You, H.; Tsutsui, S.; Hameed, S.; Kannanayakal, T. J.; Chen, L.; Xia, P.; Engbers, J. D.; Lipton, S. A.; Stys, P. K.; Zamponi, G. W. Abeta neurotoxicity depends on interactions between copper ions, prion protein, and N-methyl-D-aspartate receptors. *Proc. Natl. Acad. Sci. U. S. A.* **2012**, *109* (5), 1737−42.

(20) Moya, K. L.; Sales, N.; Hassig, R.; Creminon, C.; Grassi, J.; Di Giamberardino, L. Immunolocalization of the cellular prion protein in normal brain. *Microsc. Res. Tech.* **2000**, *50* (1), 58−65.

(21) Wulf, M.-A.; Senatore, A.; Aguzzi, A. The biological function of the cellular prion protein: an update. *BMC Biol.* **2017**, *15* (1). DOI: 10.1186/s12915-017-0375-5

(22) Gasperini, L.; Meneghetti, E.; Pastore, B.; Benetti, F.; Legname, G. Prion protein and copper cooperatively protect neurons by modulating NMDA receptor through S-nitrosylation. *Antioxid. Redox Signaling* **2015**, *22* (9), 772−84.

(23) Hansen, K. B.; Yi, F.; Perszyk, R. E.; Furukawa, H.; Wollmuth, L. P.; Gibb, A. J.; Traynelis, S. F. Structure, function, and allosteric modulation of NMDA receptors. *J. Gen. Physiol.* **2018**, *150* (8), 1081−1105.

(24) Baez, M. V.; Cercato, M. C.; Jerusalinsky, D. A. NMDA Receptor Subunits Change after Synaptic Plasticity Induction and Learning and Memory Acquisition. *Neural Plast.* **2018**, *2018*, 1.

(25) Dong, X. X.; Wang, Y.; Qin, Z. H. Molecular mechanisms of excitotoxicity and their relevance to pathogenesis of neurodegenerative diseases. *Acta Pharmacol. Sin.* **2009**, *30* (4), 379−87.

(26) Lerdkrai, C.; Asavapanumas, N.; Brawek, B.; Kovalchuk, Y.; Mojtahedi, N.; Olmedillas Del Moral, M.; Garaschuk, O. Intracellular Ca(2+) stores control in vivo neuronal hyperactivity in a mouse model of Alzheimer's disease. *Proc. Natl. Acad. Sci. U. S. A.* **2018**, *115* (6), E1279−E1288.

(27) Haberman, R. P.; Branch, A.; Gallagher, M. Targeting Neural Hyperactivity as a Treatment to Stem Progression of Late-Onset Alzheimer's Disease. *Neurotherapeutics* **2017**, *14* (3), 662−676.
(28) Dou, K. X.; Tan, M. S.; Tan, C. C.; Cao, X. P.; Hou, X. H.; Guo, Q. H.; Tan, L.; Mok, V.; Yu, J. T. Comparative safety and effectiveness of cholinesterase inhibitors and memantine for Alzheimer's disease: a network meta-analysis of 41 randomized controlled trials. *Alzheimer's Res. Ther.* **2018**, *10* (1), 126.
(29) Khosravani, H.; Zhang, Y.; Tsutsui, S.; Hameed, S.; Altier, C.; Hamid, J.; Chen, L.; Villemaire, M.; Ali, Z.; Jirik, F. R.; Zamponi, G. W. Prion protein attenuates excitotoxicity by inhibiting NMDA receptors. *J. Cell Biol.* **2008**, *181* (3), 551−65.
(30) Hodgkinson, V. L.; Zhu, S.; Wang, Y.; Ladomersky, E.; Nickelson, K.; Weisman, G. A.; Lee, J.; Gitlin, J. D.; Petris, M. J. Autonomous requirements of the Menkes disease protein in the nervous system. *Am. J. Physiol. Cell Physiol.* **2015**, *309* (10), C660−8.
(31) Faller, P.; Hureau, C. Bioinorganic chemistry of copper and zinc ions coordinated to amyloid-beta peptide. *Dalton Trans.* **2009**, No. 7, 1080−94.
(32) Drew, S. C.; Barnham, K. J. The heterogeneous nature of Cu2+ interactions with Alzheimer's amyloid-beta peptide. *Acc. Chem. Res.* **2011**, *44* (11), 1146−55.
(33) Millhauser, G. L. Copper and the prion protein: methods, structures, function, and disease. *Annu. Rev. Phys. Chem.* **2007**, *58*, 299−320.
(34) Quintanar, L.; Rivillas-Acevedo, L.; Grande-Aztatzi, R.; Gómez-Castro, C. Z.; Arcos-López, T.; Vela, A. Copper coordination to the prion protein: Insights from theoretical studies. *Coord. Chem. Rev.* **2013**, *257* (2), 429−444.
(35) Alies, B.; Renaglia, E.; Rozga, M.; Bal, W.; Faller, P.; Hureau, C. Cu(II) affinity for the Alzheimer's peptide: tyrosine fluorescence studies revisited. *Anal. Chem.* **2013**, *85* (3), 1501−8.
(36) Jones, C. E.; Klewpatinond, M.; Abdelraheim, S. R.; Brown, D. R.; Viles, J. H. Probing copper^{2+} binding to the prion protein using diamagnetic nickel^{2+} and 1H NMR: the unstructured N terminus facilitates the coordination of six copper^{2+} ions at physiological concentrations. *J. Mol. Biol.* **2005**, *346* (5), 1393−407.
(37) Walter, E. D.; Chattopadhyay, M.; Millhauser, G. L. The affinity of copper binding to the prion protein octarepeat domain: evidence for negative cooperativity. *Biochemistry* **2006**, *45* (43), 13083−92.
(38) Klewpatinond, M.; Davies, P.; Bowen, S.; Brown, D. R.; Viles, J. H. Deconvoluting the Cu^{2+} binding modes of full-length prion protein. *J. Biol. Chem.* **2008**, *283* (4), 1870−81.
(39) Chattopadhyay, M.; Walter, E. D.; Newell, D. J.; Jackson, P. J.; Aronoff-Spencer, E.; Peisach, J.; Gerfen, G. J.; Bennett, B.; Antholine, W. E.; Millhauser, G. L. The octarepeat domain of the prion protein binds Cu(II) with three distinct coordination modes at pH 7.4. *J. Am. Chem. Soc.* **2005**, *127* (36), 12647−56.
(40) Sánchez-López, C.; Rivillas-Acevedo, L.; Cruz-Vásquez, O.; Quintanar, L. Methionine 109 plays a key role in Cu(II) binding to His111 in the 92−115 fragment of the human prion protein. *Inorg. Chim. Acta* **2018**, *481*, 87−97.
(41) Grande-Aztatzi, R.; Rivillas-Acevedo, L.; Quintanar, L.; Vela, A. Structural Models for Cu(II) Bound to the Fragment 92−96 of the Human Prion Protein. *J. Phys. Chem. B* **2013**, *117* (3), 789−799.
(42) Rivillas-Acevedo, L.; Grande-Aztatzi, R.; Lomelí, I.; García, J. E.; Barrios, E.; Teloxa, S.; Vela, A.; Quintanar, L. Spectroscopic and Electronic Structure Studies of Copper(II) Binding to His111 in the Human Prion Protein Fragment 106−115: Evaluating the Role of Protons and Methionine Residues. *Inorg. Chem.* **2011**, *50* (5), 1956−1972.
(43) Chen, S. G.; Teplow, D. B.; Parchi, P.; Teller, J. K.; Gambetti, P.; Autilio-Gambetti, L. Truncated forms of the human prion protein in normal brain and in prion diseases. *J. Biol. Chem.* **1995**, *270* (32), 19173−80.
(44) Laffont-Proust, I.; Faucheux, B. A.; Hassig, R.; Sazdovitch, V.; Simon, S.; Grassi, J.; Hauw, J. J.; Moya, K. L.; Haik, S. The N-terminal cleavage of cellular prion protein in the human brain. *FEBS Lett.* **2005**, *579* (28), 6333−7.
(45) McDonald, A. J.; Dibble, J. P.; Evans, E. G.; Millhauser, G. L. A new paradigm for enzymatic control of alpha-cleavage and beta-cleavage of the prion protein. *J. Biol. Chem.* **2014**, *289* (2), 803−13.
(46) Linsenmeier, L.; Altmeppen, H. C.; Wetzel, S.; Mohammadi, B.; Saftig, P.; Glatzel, M. Diverse functions of the prion protein - Does proteolytic processing hold the key? *Biochim. Biophys. Acta, Mol. Cell Res.* **2017**, *1864* (11), 2128−2137.
(47) Sánchez-López, C.; Fernández, C. O.; Quintanar, L. Neuroprotective alpha-cleavage of the human prion protein significantly impacts Cu(ii) coordination at its His111 site. *Dalton Trans.* **2018**, *47* (28), 9274−9282.
(48) Trujano-Ortiz, L. G.; Gonzalez, F. J.; Quintanar, L. Redox cycling of copper-amyloid beta 1−16 peptide complexes is highly dependent on the coordination mode. *Inorg. Chem.* **2015**, *54* (1), 4−6.
(49) Garnett, A. P.; Viles, J. H. Copper Binding to the Octarepeats of the Prion Protein. *J. Biol. Chem.* **2003**, *278* (9), 6795−6802.
(50) Magrì, A.; Di Natale, G.; Rizzarelli, E. Copper-assisted interaction between amyloid-β and prion: Ternary metal complexes with Aβ N-terminus and octarepeat. *Inorg. Chim. Acta* **2018**, *472*, 93−102.
(51) Schlief, M. L. NMDA Receptor Activation Mediates Copper Homeostasis in Hippocampal Neurons. *J. Neurosci.* **2005**, *25* (1), 239−246.
(52) Kardos, J.; Kovacs, I.; Hajos, F.; Kalman, M.; Simonyi, M. Nerve endings from rat brain tissue release copper upon depolarization. A possible role in regulating neuronal excitability. *Neurosci. Lett.* **1989**, *103* (2), 139−44.
(53) Huang, S.; Chen, L.; Bladen, C.; Stys, P. K.; Zamponi, G. W. Differential modulation of NMDA and AMPA receptors by cellular prion protein and copper ions. *Mol. Brain* **2018**, *11* (1), 62.
(54) Nguyen, X. T. A.; Tran, T. H.; Cojoc, D.; Legname, G. Copper Binding Regulates Cellular Prion Protein Function. *Mol. Neurobiol.* **2019**, *56* (9), 6121−6133.
(55) Nishida, N.; Katamine, S.; Shigematsu, K.; Nakatani, A.; Sakamoto, N.; Hasegawa, S.; Nakaoke, R.; Atarashi, R.; Kataoka, Y.; Miyamoto, T. Prion protein is necessary for latent learning and long-term memory retention. *Cell. Mol. Neurobiol.* **1997**, *17* (5), 537−45.
(56) Leighton, P. L. A.; Nadolski, N. J.; Morrill, A.; Hamilton, T. J.; Allison, W. T. An ancient conserved role for prion protein in learning and memory. *Biol. Open* **2018**, *7* (1). DOI: 10.1242/bio.025734
(57) Maureira, C.; Letelier, J. C.; Alvarez, O.; Delgado, R.; Vergara, C. Copper enhances cellular and network excitabilities, and improves temporal processing in the rat hippocampus. *European Journal of Neuroscience* **2015**, *42* (12), 3066−3080.
(58) Gaier, E. D.; Rodriguiz, R. M.; Zhou, J.; Ralle, M.; Wetsel, W. C.; Eipper, B. A.; Mains, R. E. In vivo and in vitro analyses of amygdalar function reveal a role for copper. *J. Neurophysiol.* **2014**, *111* (10), 1927−1939.
(59) Cirrito, J. R.; Yamada, K. A.; Finn, M. B.; Sloviter, R. S.; Bales, K. R.; May, P. C.; Schoepp, D. D.; Paul, S. M.; Mennerick, S.; Holtzman, D. M. Synaptic Activity Regulates Interstitial Fluid Amyloid-β Levels In Vivo. *Neuron* **2005**, *48* (6), 913−922.
(60) Bateman, R. J.; Munsell, L. Y.; Morris, J. C.; Swarm, R.; Yarasheski, K. E.; Holtzman, D. M. Human amyloid-β synthesis and clearance rates as measured in cerebrospinal fluid in vivo. *Nat. Med.* **2006**, *12* (7), 856−861.
(61) Schilling, K. M.; Tao, L.; Wu, B.; Kiblen, J. T. M.; Ubilla-Rodriguez, N. C.; Pushie, M. J.; Britt, R. D.; Roseman, G. P.; Harris, D. A.; Millhauser, G. L. Both N-Terminal and C-Terminal Histidine Residues of the Prion Protein Are Essential for Copper Coordination and Neuroprotective Self-Regulation. *J. Mol. Biol.* **2020**, *432* (16), 4408−4425.
(62) Taylor, D. R.; Watt, N. T.; Perera, W. S. S.; Hooper, N. M. Assigning functions to distinct regions of the N-terminus of the prion protein that are involved in its copper-stimulated, clathrin-dependent endocytosis. *J. Cell Sci.* **2005**, *118* (21), 5141−5153.

https://doi.org/10.1021/acs.inorgchem.1c00846
Inorg. Chem. XXXX, XXX, XXX−XXX

(63) Hooper, N. M.; Taylor, D. R.; Watt, N. T. Mechanism of the metal-mediated endocytosis of the prion protein. *Biochem. Soc. Trans.* **2008**, *36* (6), 1272−1276.
(64) Caetano, F. A.; Lopes, M. H.; Hajj, G. N. M.; Machado, C. F.; Pinto Arantes, C.; Magalhaes, A. C.; Vieira, M. D. P. B.; Americo, T. A.; Massensini, A. R.; Priola, S. A.; Vorberg, I.; Gomez, M. V.; Linden, R.; Prado, V. F.; Martins, V. R.; Prado, M. A. M. Endocytosis of Prion Protein Is Required for ERK1/2 Signaling Induced by Stress-Inducible Protein 1. *J. Neurosci.* **2008**, *28* (26), 6691−6702.
(65) Coitinho, A. S.; Lopes, M. H.; Hajj, G. N. M.; Rossato, J. I.; Freitas, A. R.; Castro, C. C.; Cammarota, M.; Brentani, R. R.; Izquierdo, I.; Martins, V. R. Short-term memory formation and long-term memory consolidation are enhanced by cellular prion association to stress-inducible protein 1. *Neurobiol. Dis.* **2007**, *26* (1), 282−290.
(66) Klewpatinond, M.; Viles, J. H. Empirical rules for rationalising visible circular dichroism of Cu2+and Ni2+histidine complexes: Applications to the prion protein. *FEBS Lett.* **2007**, *581* (7), 1430−1434.
(67) Stanyon, H. F.; Cong, X.; Chen, Y.; Shahidullah, N.; Rossetti, G.; Dreyer, J.; Papamokos, G.; Carloni, P.; Viles, J. H. Developing predictive rules for coordination geometry from visible circular dichroism of copper(II) and nickel(II) ions in histidine and amide main-chain complexes. *FEBS J.* **2014**, *281* (17), 3945−3954.
(68) Liebert, A.; Bicknell, B.; Adams, R. Prion Protein Signaling in the Nervous System—A Review and Perspective. *Signal Transduction Insights* **2014**, *3*, 3.
(69) Um, J. W.; Nygaard, H. B.; Heiss, J. K.; Kostylev, M. A.; Stagi, M.; Vortmeyer, A.; Wisniewski, T.; Gunther, E. C.; Strittmatter, S. M. Alzheimer amyloid-β oligomer bound to postsynaptic prion protein activates Fyn to impair neurons. *Nat. Neurosci.* **2012**, *15* (9), 1227−1235.
(70) Liu, L.; Jiang, D.; McDonald, A.; Hao, Y.; Millhauser, G. L.; Zhou, F. Copper redox cycling in the prion protein depends critically on binding mode. *J. Am. Chem. Soc.* **2011**, *133* (31), 12229−37.
(71) Martiška, L.; Husáriková, L.; Repická, Z.; Valigura, D.; Valko, M.; Mazúr, M. EPR Study of 5-Chlorosalicylate-Cu(II)-3-Pyridylmethanol Ternary Complex Systems in Frozen Water-Methanol Solutions. *Appl. Magn. Reson.* **2010**, *39* (4), 423−435.
(72) Drew, S. C.; Noble, C. J.; Masters, C. L.; Hanson, G. R.; Barnham, K. J. Pleomorphic copper coordination by Alzheimer's disease amyloid-beta peptide. *J. Am. Chem. Soc.* **2009**, *131* (3), 1195−207.
(73) Mange, A.; Milhavet, O.; Umlauf, D.; Harris, D.; Lehmann, S. PrP-dependent cell adhesion in N2a neuroblastoma cells. *FEBS Lett.* **2002**, *514* (2−3), 159−62.
(74) Viegas, P.; Chaverot, N.; Enslen, H.; Perriere, N.; Couraud, P. O.; Cazaubon, S. Junctional expression of the prion protein PrPC by brain endothelial cells: a role in trans-endothelial migration of human monocytes. *J. Cell Sci.* **2006**, *119* (22), 4634−4643.
(75) Haigh, C. L.; Lewis, V. A.; Vella, L. J.; Masters, C. L.; Hill, A. F.; Lawson, V. A.; Collins, S. J. PrP^{C}-related signal transduction is influenced by copper, membrane integrity and the alpha cleavage site. *Cell Res.* **2009**, *19* (9), 1062−78.
(76) Klemm, J. D.; Schreiber, S. L.; Crabtree, G. R. Dimerization as a Regulatory Mechanism in Signal Transduction. *Annu. Rev. Immunol.* **1998**, *16* (1), 569−592.

https://doi.org/10.1021/acs.inorgchem.1c00846
Inorg. Chem. XXXX, XXX, XXX−XXX